PERGAMON

Aerosol Science 34 (2003) 1323–1346

Journal of
Aerosol Science

www.elsevier.com/locate/jaerosci

Single particle MS, SNMS, SIMS, XPS, and FTIR spectroscopic analysis of soot particles during the AIDA campaign

U. Kirchner[a,*], R. Vogt[a], C. Natzeck[b], J. Goschnick[b]

[a] *Ford Forschungszentrum Aachen GmbH, Süsterfeldstraße 200, D-52072 Aachen, Germany*
[b] *Forschungszentrum Karlsruhe GmbH, IFIA, Postfach 3640, D-76021 Karlsruhe, Germany*

Received 7 February 2002; accepted 11 November 2002

Abstract

Within the framework of the AIDA soot aerosol campaign diesel soot particles, spark generated soot particles, and aerosol mixtures were characterized with respect to their chemical state using different surface sensitive analysis methods. A comparison between diesel soot and graphite spark generated soot revealed a significant difference in the chemical composition of the particle surfaces. No distinct change from external to internal mixing could be detected by single particle mass spectrometry for mixtures of diesel soot and $(NH_4)_2SO_4$ aerosol since the spectra of diesel soot and $(NH_4)_2SO_4$ aerosol were surprisingly similar due to sulfate on the surface of diesel soot particles and traces of carbon impurities on ammonium sulfate particles. In addition to the expected formation of new particles a considerable change of the soot particle surface was detected while exposing diesel soot or spark generated soot to α-pinene and ozone, indicating a surface layer formed by oxidation products of α-pinene. However, the oxygen-containing hydrocarbon fragments detected by single particle mass spectrometry were distinctly different for the two soot types, which can be explained by either the different product adsorption or ionization behavior. Depositions of α-pinene reaction products on the surface could be confirmed by QMS-SIMS and XPS for particles of both types of soot. Due to the high mass resolution of TOF-SIMS acidic derivatives were identified as reaction products of α-pinene and ozone. The analytical methods applied in this work elucidated the different properties of spark generated soot compared to diesel soot. Therefore, spark generated soot should only be used with care as a general diesel soot surrogate.

Keywords: Heterogeneous chemistry; Soot; Aerosol; SNMS; SIMS

* Corresponding author. Tel.: +49-241-9421-217; fax:+49-241-9421-414.
E-mail address: ukirchne@ford.com (U. Kirchner).

0021-8502/$ - see front matter © 2003 Elsevier Ltd. All rights reserved.
doi:10.1016/S0021-8502(03)00362-8

1. Introduction

Atmospheric aerosols are subject of experimental and theoretical investigations due to their ubiquitous occurrence and their strong interaction with the ambient atmosphere. In urban areas soot aerosol is of particular interest. It is produced by e.g. industrial processes, combustion engines, and the burning of carbon-containing material for household heating. In many laboratory investigations graphite spark generated soot has been used as a soot aerosol surrogate (Ammann et al., 1998; Kotzick, Panne, & Niessner, 1997; Weingartner, Burtscher, & Baltensperger, 1997; Kamm, Möhler, Naumann, Saathoff, & Schurath, 1999; Kirchner, Börensen, Scheer, & Vogt, 1999). Conclusions for the atmosphere have been drawn under the assumption that spark generated soot has a similar behavior as atmospheric soot. However, a difference in the hydration behavior of spark generated soot and diesel soot has already been reported (Weingartner et al., 1997). In order to validate or refute the suitability of spark generated soot as a diesel soot surrogate, and to investigate the properties of real diesel soot the AIDA measurement campaign was carried out.

Ambient aerosol usually consists of more than one compound. Therefore, multicomponent aerosols were also investigated during this campaign: (a) the transition from an external to an internal mixture of soot and ammonium sulfate, and (b) coating of soot by reaction products of α-pinene and ozone. The coating of diesel soot and spark generated soot were studied and their behavior is compared.

Heterogeneous atmospheric reactions take place on the surface of particles. Therefore, surface sensitive methods were employed. In situ single particle mass spectrometric analyses were performed with the LAMPAS-2 system (Laser Mass Analyzer for Particles in the Airborne State). The laser desorption and ionization, which was used in the instrument has been shown to leave the core of single particles intact (Weiss, Verheijen, Marijnissen, & Scarlett, 1997). Also samples of soot particles were investigated with further surface sensitive analysis methods, such as plasma-based Secondary Neutral Mass Spectrometry (SNMS), with a quadrupole mass spectrometer Secondary Ion Mass Spectrometry (QMS-SIMS), Time-of-Flight Mass Spectrometry (TOF-SIMS) and X-ray excited Photoelectron Spectroscopy (XPS). For all the off-line analyses the particles were collected by a Berner cascade impactor with rotating impaction plates to obtain a homogenous spread of a monolayer of particles on an indium foil.

2. Experimental

2.1. Experimental facility and sample collection

Experiments were carried out in the 84 m^3 aerosol chamber AIDA at the Forschungszentrum Karlsruhe, Germany. A detailed description of the chamber facility, its instrumentation, and the aerosol generation is given by Saathoff et al. (2003a).

Soot was either produced by a graphite spark discharge generator (model GfG 1000, Palas GmbH, Germany; "GfG soot") or by a diesel engine (4-cylinder Volkswagen TDI 1.9 L, type 1Z, 66 kW, intake air cooling, direct fuel injection, turbocharged, exhaust gas recirculation, oxidation catalyst, eddy current break). The spark generator was operated with 99.999% Ar as carrier gas for the discharge. The engine was operated at steady state and controlled load (17 kW at 2500 rpm). The exhaust was diluted 1:10 and passed through three denuders of mole sieve, activated charcoal, and

cobalt oxide to remove water, hydrocarbons, and nitrogen oxides. $(NH_4)_2SO_4$ aerosol was produced from an aqueous solution, which was nebulized and subsequently passed through a diffusion dryer.

For the single particle mass spectrometer the particles were sampled through a 2 m long and 7 mm inner diameter stainless steel tube with a flow of 1.61 min^{-1}. Filter samples for infrared analysis were collected on 47 mm Teflon filters (pore size 0.2 μm, Sartorius, Germany) and stored in glass petri dishes.

Offline surface analysis of diesel soot and spark generated soot particles was obtained by SNMS, QMS-SIMS, TOF-SIMS and XPS. The samples were taken directly out of the AIDA chamber or behind the spark generator, or the diesel engine. Diesel soot particles were sampled before and after passing the denuders. The particles were collected on indium foils of high-grade purity (99, 999 wt%, GOODFELLOW) using a Berner cascade impactor with eleven rotary impaction plates (Berner & Klaus, 1985). A throughput of 25 l/min was applied to separate the particles in various size ranges corresponding to their aerodynamic diameter. According to the manufacturer's certificate for latex spheres the average aerodynamic diameters for the stages 1–4 amount to 25, 50, 100, 200 nm, respectively. The soot particles sampled behind the spark generator or the diesel engine were deposited as agglomerates on the first two stages (see Wentzel, Gorzawski, Naumann, Saathoff, & Weinsbruch, 2003). However, those samples of both sorts of soot that were taken out of the AIDA chamber during the coating experiments were distributed on the stages 1–4. Each time samples of two stages were examined with the highest coverage on the indium foil (approximately 10% during coating experiments, approximately 25% directly after the soot sources).

2.2. Description of the LAMPAS-2 Single Particle Mass Spectrometer

In collaboration with Spengler and his research group (University of Würzburg and Giessen, Germany) and Inbitec GmbH (Berlin, Germany) the "Laser Mass Analyzer for Particles in the Airborne State" (LAMPAS-2) was designed as a portable system for physical and chemical analysis of single aerosol particles in the size range 0.2–10 μm. The instrument was described by Trimborn, Hinz, and Spengler (2000). Briefly, the instrument utilizes Laser Desorption Ionization (LDI) to vaporize and ionize material from individual aerosol particles. The complete system is mounted in a movable rack on wheels with a size of 174 × 84 × 121 cm (length × width × height). The total weight is about 300 kg, allowing convenient transportation in a van. The rack includes all control devices for the optics, the mass spectrometer and the vacuum system. The rack construction ensures high stability and vibration compensation.

For chemical analysis and concurrent aerodynamic-size determination the aerosol enters the instrument through a differentially pumped inlet system. It is designed to efficiently separate particles from the gas fraction of the aerosol and to reduce the pressure from atmospheric to 3×10^{-6} mbar, which is the working pressure of the time-of-flight mass spectrometer. The inlet allows efficient transmission of particles in the aerodynamic diameter range from 200 nm up to 10 μm.

After passing the aerosol inlet, the particles cross a continuous laser beam (532 nm, Nd:YVO4 laser) indicating their presence as a light scattering signal. The scatter light signal is used to trigger a pulsed ionization laser (337 nm, N_2 laser) (Fig. 1). A particle, which is hit by the ionization laser beam is partially vaporized and ionized. The positive and negative ions are analyzed simultaneously by a bipolar time-of-flight mass spectrometer with a resolution of $m/\Delta m \approx 400$. Spectra are

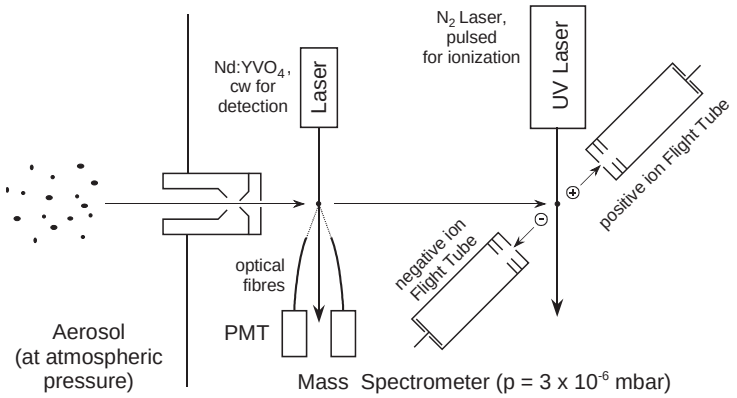

Fig. 1. Schematic diagram of the single particle mass spectrometer: particle detection and ionization. Sizes and distances, especially between inlet, particle detection laser and ionization laser are not drawn to scale.

recorded by a dual-channel digital oscilloscope (LeCroy, Model 9354A, Chestnut Ridge, NY) and are transferred to a personal computer for data processing and storage.

The size of the detected particles is varied by changing the delay time between the scattered light pulse and firing of the ionization laser. Data processing of hundreds of spectra of single particles was performed by a fuzzy clustering algorithm (Hinz, Greweling, Drews, & Spengler, 1999). For each particle size, spectra with similar main components are sorted into up to 10 classes and the spectral patterns present averages of all MS-spectra in the corresponding class. Sampling usually started immediately after filling of the chamber and typical sampling times are 30–60 min for each size, so that all spectral patterns are averages over these time periods.

2.3. FTIR analysis of aerosol samples

All infrared spectra were measured at 4 cm^{-1} resolution using a Bruker Equinox 55 Fourier Transform Infrared (FTIR) Spectrometer equipped with a Mercury-Cadmium-Telluride detector. The aerosol samples were collected on 47 mm Teflon filters and transferred to 25 mm diameter KBr optical windows. The filters were placed upside down on freshly cleaned windows and a petri dish was taken to gently rub on the rear side of the filter. The filter was carefully taken off leaving the soot as a homogeneous film on the optical window. Transmission spectra were recorded relative to the freshly cleaned KBr windows as reference. All spectra are averages of 100 scans in the typical wave number range from 4000 to 6000 cm^{-1}.

2.4. Surface analysis of particles by secondary mass spectrometry

2.4.1. Plasma-based secondary neutral mass spectrometry (SNMS) and secondary ion mass spectrometry with quadrupole mass analyzer (QMS-SIMS)

A detailed surface analysis of the particles was performed with an INA-3 system (SPECS GmbH, Berlin), which is suitable for plasma-based SNMS as well as SIMS measurements (see Fig. 2). Details of this system are described elsewhere (Jede, Seifert, & Dünnebier, 1987). To determine the

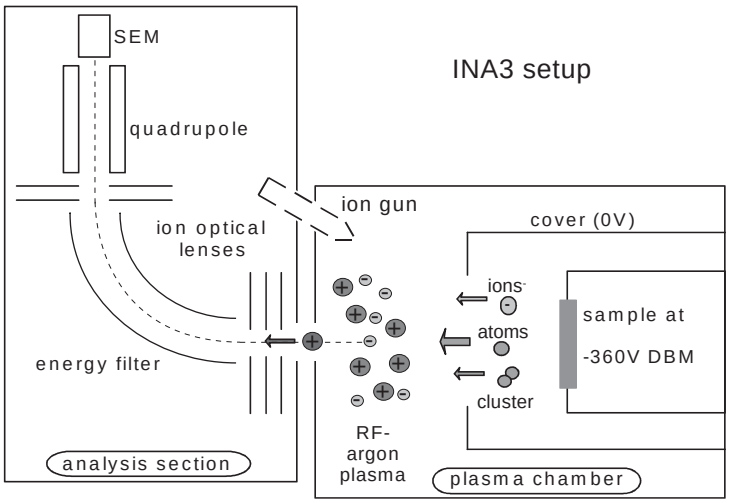

Fig. 2. Schematic diagram of the INA3 instrument for plasma-based Secondary Neutral Mass Spectrometry (plasma-based SNMS) and Secondary Ion Mass Spectrometry both coupled to a quadrupole mass analyzer.

total elemental inventory of the particles plasma-based SNMS was applied. The sample is positioned behind an orifice in front of an argon plasma. A negative potential is applied to the carrier foil, which extracts argon ions out of the plasma and accelerates them towards the sample. The applied target potential of 360 V and the plasma potential of about 40 V, provides argon ions of 400 eV to bombard the sample with a current density of about 1 mA/cm^2. The sputtered area of the sample was 38.5 mm^2. The eroded material predominantly consists of neutral atoms, which become partially ionized by electron impact in the plasma. Subsequently, the post-ionized neutrals are energy-filtered, mainly in order to discriminate thermal species. A quadrupole mass filter which was able to resolve one mass was used for mass analysis. The geometrical arrangement of the INA-3 with its coalignment of bombardment direction and spectrometer entrance axis perpendicular to the sample surface is especially advantageous for particle analysis as shadowing effects are avoided. An erosion rate of 2 nm/s was found to be appropriate in earlier investigations for depth profiles of airborne particles with a size of about 100 nm (Bentz, Ewinger, Goschnick, Kannen, & Ache, 1993). Because of the high average erosion rate and the small size of the particles in the 100 nm range the mass span was chosen to cover 0 to 120 amu. The total registration time for all relevant elements amounted to 300 s resulting in an analyzed depth range of more than 600 nm after erosion start. This corresponds to several particle diameters and assures the complete particles inventory to be analyzed. Depth profiles of the particles could be recorded with a depth resolution of about 20 nm (Goschnick, Schuricht, Schweicker, & Ache, 1993; Goschnick, Schuricht, & Ache, 1994). The samples were cooled to slightly below 0°C by a moderate liquid nitrogen flow.

For the QMS-SIMS analysis the plasma was switched off. A separate ion gun was used for the bombardment with argon ions of higher ion energy compared with SNMS (5 keV, current density 10 μA/cm^2). This is advantageous to increase the intensities of molecular ions, which form the database for further chemical characterization. Because of the low current density of the bombardment no cooling was necessary to keep the samples at room temperature. The erosion rate

was approximately 0.05 nm/s according to former investigations. Hence, the recording time of the spectra of 540 s corresponds to an analyzed depth of about 30 nm. The signals of 16 masses can be recorded in depth profile mode.

2.4.2. Secondary ion mass spectrometry with time-of-flight instrumentation (TOF-SIMS)

Selected samples were additionally analyzed using a time-of-flight mass spectrometer (TOF-MS) with a Ga^+ liquid metal ion source of approximately 100 nm beam width (ION-TOF/University Münster, Germany). Due to the very low bombardiers ion current of 10 nA/cm^2 less than 1% (about 1×10^{12} atoms/cm^2) of the top monolayer is removed and can be analyzed. Therefore, under static conditions nearly all secondary ions originate from bombardment of unaffected areas. Although principally possible, the conglomerate of compounds usually contained in the aerosol particles prohibits the identification of molecular ions of the whole stoichiometric unit. Therefore, the signal of small molecular fragments was preferred for the characterization of compounds. The high mass resolution of about $m/\Delta m = 5000$ allows mostly an unequivocal assignment of the fragments to the mass signals. The high useful yield of the TOF-MS instrument is required to detect the low number of secondary ions coming off the small area illuminated by the narrow beam width of the ion gun. The measurement was performed with a pulsed ion source using Ga^+ of 30 kV primary energy with a pulse period of 15 ns. Integral spectra were acquired with the Ga^+ source scanned over a surface of 120×120 μm averaged over 200 s.

2.5. Photo electron spectroscopy (XPS)

X-ray Photoelectron Spectroscopy (XPS) was performed in an ESCALAB-5 surface-analytical system (VG SCIENTIFIC, East Grinstead, UK). Non-monochromatized Mg Kα radiation (100 or 200 W) was used for excitation. The spectra were recorded with a 150° hemispherical energy analyzer operated in the constant analyzer energy mode (CAE) at a pass energy of 20 eV. Due to the particle coverage of $\leqslant 50\%$ on the indium carrier foil charging problems could be prevented. The binding energy scale was calibrated in the usual way defining the carbon 1 s peak of lowest binding energy (in case of a carbon multiplet) to be at 285 eV. The multiplet analysis of relevant peaks was achieved by fitting model functions of mixed Gaussian and Lorentzian shape into the measured intensity distribution. Background subtraction was performed using Shirley's method (Shirley, 1972).

3. Characterization of neat diesel soot particles and spark generated soot particles

The AIDA aerosol chamber was filled with soot from the exhaust of the diesel engine as described in the experimental section until a soot concentration of $\sim$70 μg m^{-3} was reached. Approximately 90–95% of the water, NO_x, and hydrocarbons were removed from the exhaust by the denuders (see also Section 2.1.) was estimated by comparison to a filling without the use of denuders (Saathoff et al., 2003b). The NO_x concentration in the AIDA was below $\sim$20 ppbv and the relative humidity was decreasing from 43% to 33% during experiment No. 2 at room temperature (for the measurement principles see Saathoff et al., 2003a). The humidity was decreasing during the experiment, because clean dry synthetic air was continuously supplied to the chamber to replace the sampled air volume in order to keep a constant pressure.

Soot produced by the Palas GfG spark discharge generator was diluted with moist and NO_x containing air to better match the aging conditions of diesel soot. The amount of soot in the aerosol chamber was $\sim$100 μg m^3, the NO_x concentration was $\sim$60 ppbv, and the relative humidity was from 47% to 38%.

3.1. Single particle mass spectrometry

3.1.1. Single particle mass spectra of diesel soot

Two classes of diesel soot spectra sampled directly from the aerosol chamber are displayed in Fig. 3a and b. More than 200 particles were analyzed and the spectra were sorted into 5 classes. The positive ions in Fig. 3a are dominated by signals of Na^+, K^+, and Fe^+. Negative ions, such as oxygen containing carbonaceous fragments ($C_2H_3O^-$ at 43 amu), NO_x reaction products (NO_2^- and NO_3^- at 46 and 62 amu, respectively), and sulfate fragments (HSO_4^- at 97 amu) are observed, whereas the fragments of the soot core (C_5^- at 60 amu, C_6^- at 72 amu, and C_7^- at 84 amu) are less abundant. Surface reaction products are very sensitively probed by single particle mass spectrometry (Weiss et al., 1997). Other classes of diesel spectra (Fig. 3b) contain more intense signals of sulfate (HSO_4^- at 97 amu and SO_3^- at 80 amu), smaller peaks of sodium (Na^+ at 23 amu) and virtually no signals originating from the soot core. The peak at 99 amu in the negative spectra is an artifact from oscillations occurring after very strong signals in the capacitor, which is used to separate the ion signal from the high potential of the detector. The sulfate may originate from compounds incorporated in the particles or from a layer of condensed sulfuric acid, which may obscure the underlying soot core. A fraction of 7% of the diesel soot spectra contains negative ion signals at 60 and 76 amu, which can be attributed to SiO_2^- and SiO_3^- fragments. This is consistent with transmission electron microscopy (TEM/EDX) measurements by Wentzel et al. (2003), in which also a small signal of Si was observed.

Distinctly different mass spectra are obtained from particles, which were sampled directly from the tailpipe of a diesel vehicle (Ford Mondeo Mondeo 1.8 L, turbocharged) without the use of denuders (Fig. 3c) (Kirchner, Scheer, & Vogt, 2001). In both, positive and negative ion mode fragments of carbon cluster ions C_x are observed. Most probably these ions are formed from hydrocarbons, which were not removed by a denuder. Due to the 90–95% efficiency of the denuders one would expect still some hydrocarbons adsorbed on the particle surfaces even if the adsorption/desorption equilibrium was established in the time during which the exhaust flows through the denuders. Interestingly, Ca^+ was observed in these particles as a signal, which is more intense than K^+ or Na^+, whereas in particles from the aerosol chamber the Ca^+ peak was very small or obscured by the tailing of the intense K^+ peak. Spectra of diesel soot particles from the AIDA chamber are relatively similar, the differences may be explained by more adsorbed hydro carbons (Fig. 3a) or more sulfate (Fig. 3b) on the surface of individual particles. Spectra of particles from a different engine with different exhaust aftertreatment, sampling conditions, fuel, and operating conditions are significantly less similar (Fig. 3c).

A large sulfate signal, nearly full scale, is mainly obtained from small particles (0.2 μm), whereas the signal of Fe^+ is large in bigger particles (1 μm) and is not observed in the small particles (Fig. 4). The distribution of these compounds did not change with aging for 43 h in the aerosol chamber. Therefore, it is likely that sulfate and iron are not lost or accumulated on the particles in an ongoing reaction, but are already contained in the particles as they enter the chamber. This could be explained by the high sulfur content in the diesel fuel ([S] = 385 ppm (mass/mass), analyzed by Petrolab GmbH, Speyer, Germany) used to supply the engine, and which may have been oxidized to

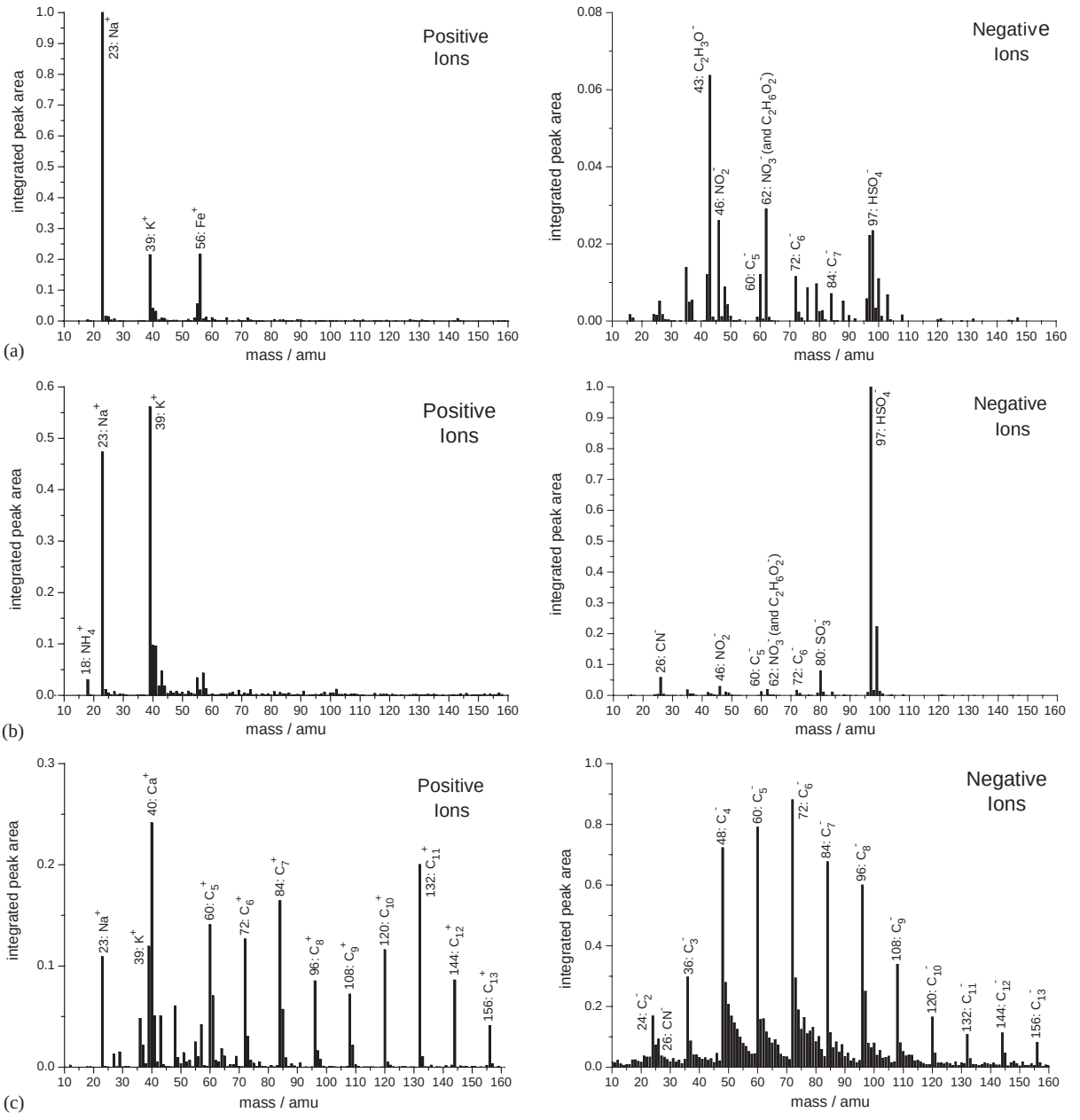

Fig. 3. (a) and (b) 2 different classes of positive and negative mass spectra of 0.5 μm diameter diesel soot particles sampled from the AIDA chamber, (c) spectrum of the most abundant class of 0.5 μm particles sampled directly at the tailpipe from the exhaust of a diesel passenger car (1.8 L, turbocharged), (d) and (e) class of positive and negative mass spectra of 0.5 μm diameter spark generated soot particles sampled from the AIDA chamber without (d) and with (e) exposure to NO_x. Ion peaks are labeled with the most probable assignments.

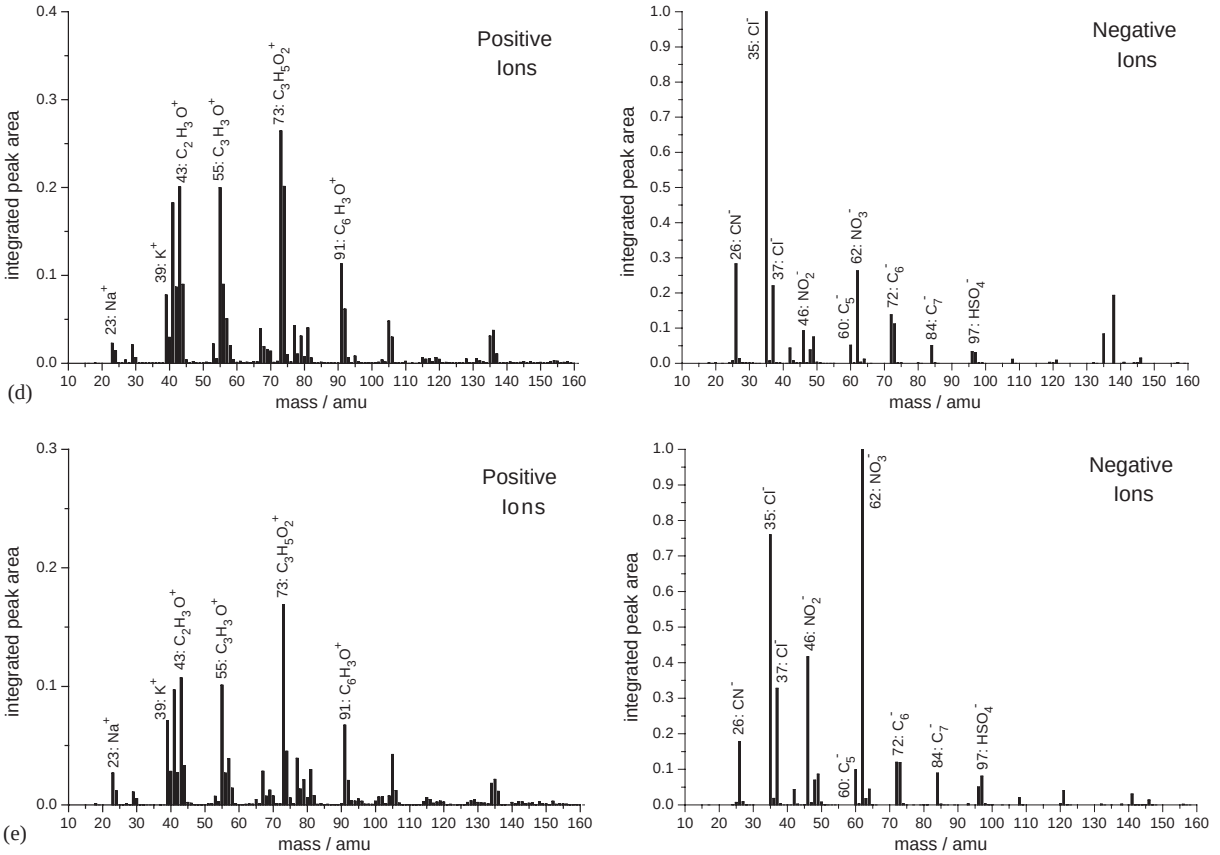

Fig. 3. Continued

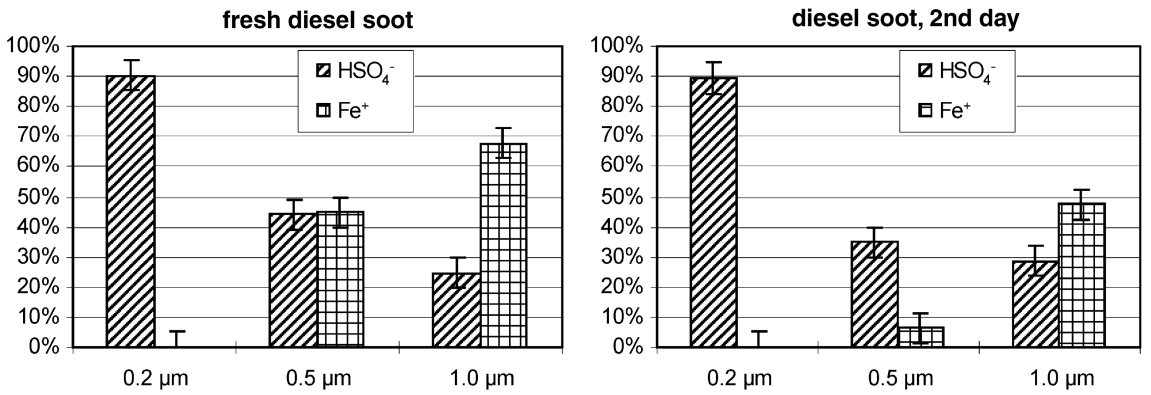

Fig. 4. Fraction of particles that contain large sulfate signals (HSO_4^- at 97 amu) and iron signals (Fe^+ at 56 amu) at different sizes and different storage times in the aerosol chamber during experiment No. 2.

sulfate and deposited on the particles. The iron is probably released by moving parts in the engine, such as the piston.

It is important to note, that integrated peak areas do not represent quantitative information of detected compounds. The peak height depends on ionization cross section, laser intensity and underlying matrix. The detection efficiencies of ammonium or iron, for example, are approximately 330 and 40 times, respectively, lower than of sodium. The detection sensitivity for chlorine is about eight times less compared to nitrate (Hinz et al., 1999). These values also depend on the characteristics of the ionization laser. For ionization by a 266 nm Nd:YAG laser the ratio of detection efficiencies for sodium to ammonium is ~70 (Gross, Gälli, Silva, & Prather, 2000).

3.1.2. Single particle mass spectra of spark generated soot

A typical class of spark generated soot spectra sampled directly from the aerosol chamber contains small signals of Na^+ and K^+, and is dominated by oxygen containing carbonaceous fragments ($C_2H_3O^+$ at 43 amu, $C_3H_3O^+$ at 55 amu, $C_3H_5O_2^+$ at 73 amu, and $C_6H_3O^+$ at 91 amu) as positive ions (Fig. 3d). Chloride (Cl^- at 35 and 37 amu), NO_x reaction products (CN^-, NO_2^- and NO_3^- at 26, 46 and 62 amu, respectively), and carbon clusters (C_5^- at 60 amu, C_6^- at 72 amu, and C_7^- at 84 amu) are observed as negative ions, whereas fragments of sulfate (HSO_4^- at 97 amu) are less abundant (Fig. 3d). No size dependence of the chemical surface composition was observed, as expected from the uniform particle formation during the spark discharge.

Spark generated soot with added NO_x yields similar spectra, but with considerably larger signals of NO_x reaction products (NO_2^- at 46 amu, and NO_3^- at 62 amu). No significant difference of the CN^- signal at 26 amu was observed (Fig. 3e). These compounds, as well as the observed oxygenated fragments may originate from impurities in the graphite electrodes of the generator and from impurities in the gas supply for the spark discharge (Kirchner et al., 2001).

The MS-spectra of diesel and spark generated soot are distinctly different, even if sampled after 2 days of residence in the aerosol chamber under similar conditions. Therefore, it may be concluded that the surfaces of both types of soot are chemically different. Since the surface is the reacting part of a particle, the reactivity of the particles may also be different. The reaction of soot with NO_2 has been found to be a factor of 6–8 slower on diesel soot than on spark generated soot (Kirchner, Scheer, & Vogt, 2000). Therefore, spark generated soot may be of limited use as a diesel soot surrogate for the investigation of atmospheric reactions and reaction rates. Hence, reaction rates obtained on spark generated soot should be taken as upper limits for atmospheric simulations. Another example for a slow reaction with soot is the loss of O_3 on soot, which has been found to be almost negligible for the atmosphere in a recent study (Kamm et al., 1999).

The amount of adsorbed surface species could not be quantified. The difference between the mass spectra of spark generated and diesel soot is too large to allow a quantitative comparison. For quantitative analysis the spectrometer needs to be calibrated for each chemical compound, because ionization efficiencies may be very different. For complex mixtures, such as the organic fraction of soot this might not be straightforward, because of the inhomogeneous ionization conditions.

3.2. FTIR spectra of diesel and spark generated soot

The difference of the sulfate content of diesel soot and spark generated soot is also observed by FTIR spectroscopy (Fig. 5). The peaks in the diesel soot spectrum at 1090 cm^{-1} and at 615 cm^{-1} are

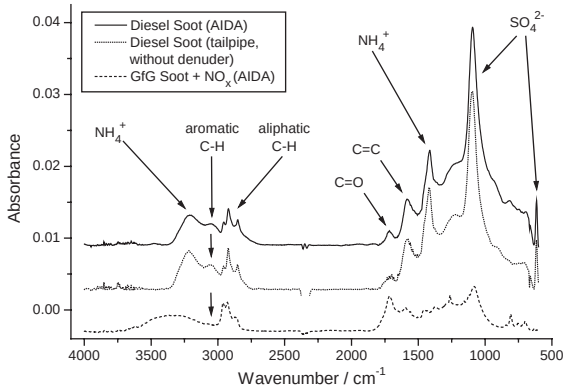

Fig. 5. FTIR spectra of spark generated soot and of diesel soot sampled from the engine tailpipe without the use of denuders and from the AIDA aerosol chamber. Diesel soot contains more sulfate than spark generated soot, which confirms the mass spectrometric results of stronger HSO_4^- signals at 97 amu. The observed ammonium may act as counter ion. Band assignments according to Schnaiter et al. (1999) and Kirchner et al. (2000).

attributed to the SO_4^{2-} ion, which has absorption bands at 1130–1080 cm^{-1} and at 680–610 cm^{-1}. Due to the observed peaks at 3210 and 1415 cm^{-1}, the counter ion is supposed to be ammonium, which has absorption bands at 3335–3030 cm^{-1} and at 1485–1390 cm^{-1}. There is only a minor NH_4^+ peak at 18 amu in some of the mass spectra, because of its low MS sensitivity. The detection efficiency of ammonium as NH_4^+ at the laser light wavelength of 337 nm is approximately a factor of ~330 lower than of sodium as Na^+ (Hinz et al., 1999). No ammonium or significant sulfate signals are observed in mass spectra or FTIR spectra of spark generated soot. In good agreement with Schnaiter et al. (2003) a stronger band of aromatic C–H at 3050 cm^{-1} was observed in diesel soot than in spark generated soot samples.

The infrared spectra of diesel soot, which was sampled before and after the denuder do not display any differences and are very similar as if sampled directly out of the AIDA chamber (Fig. 5). The mass spectra of particles from the AIDA chamber are clearly different compared to tailpipe particles from the Ford vehicle (Fig. 3). The difference in the mass spectra may be caused by a very thin layer on the particle surface that is too thin to contribute significantly to the infrared spectrum. Since FTIR aerosol analysis probes bulk aerosol composition and single particle analysis is more surface sensitive, the latter is more sensitive to trace gas chemistry occurring with/without denuders in place. Additionally, the soot particles originate from two different engines, which may not be comparable as discussed above.

3.3. Plasma-based SNMS and QMS-SIMS analysis of diesel soot and spark generated soot

First, soot particles were investigated that were sampled as described in Section 2.1 from the spark generator or at the diesel engine test stand before and after passing the denuders.

SNMS spectra were acquired of these samples over a depth range of more than one particle diameter to assure an integral analysis of the whole particles. The obtained elemental inventory of the particles is shown in Fig. 6a. As expected for soot particles both, spark generated and diesel soot, contain the elements carbon and carbon-bound hydrogen. Further, sulfur, chlorine, potassium and

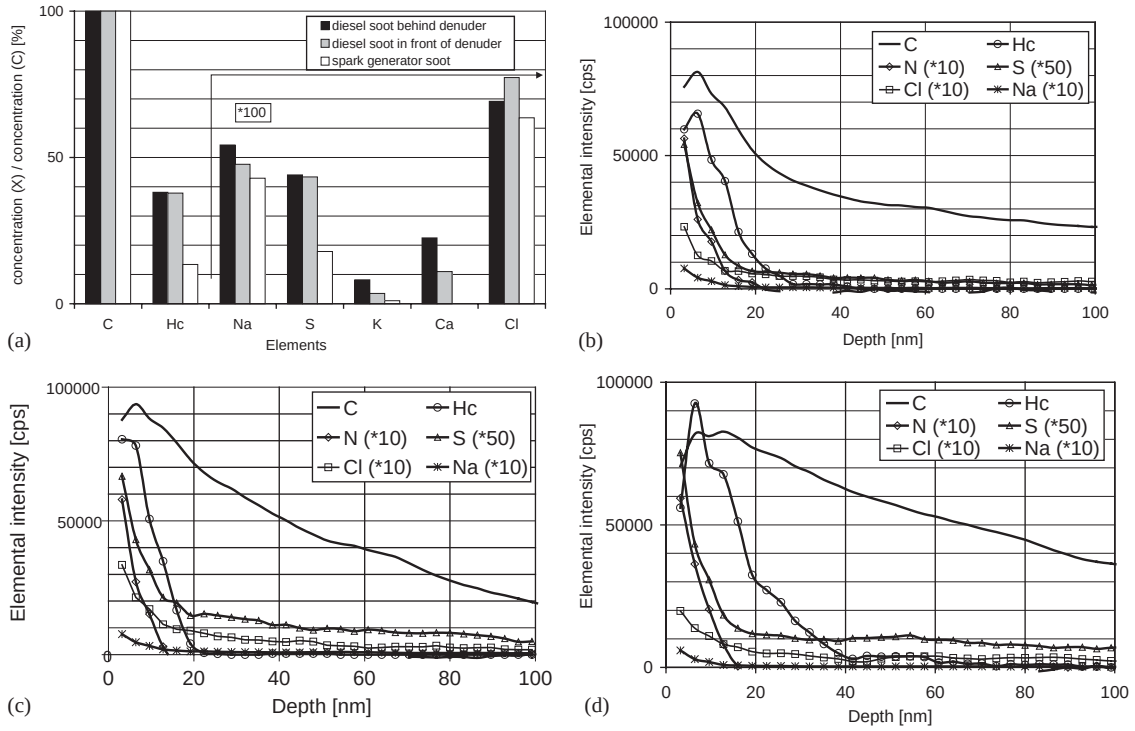

Fig. 6. SNMS spectra of diesel soot and spark generated soot particles sampled directly at the source: (a) elemental inventory of whole particles; (b) depth profiles of spark generated soot; (c) depth profiles of diesel soot; (d) depth profile of diesel soot sampled behind the denuder. Sputter time was converted into a depth scale with an erosion rate of 2 nm/s for the soot particles.

calcium could be detected. Carbon-bound hydrogen was calculated from the ratio of the intensities on the mass 13 amu (cluster signal CH^+) and the elemental signal on mass 12 amu (C^+) (Ewinger, Goschnick, & Ache, 1991).

In comparison to spark generated soot the diesel soot particles show a considerably higher ratio of sulfur to carbon (see Fig. 6a). This finding corresponds to the high sulfur content of the diesel fuel, which was used. Likewise the concentration of carbon-bound hydrogen (Hc) and calcium to carbon ratio is higher in diesel soot than in the spark generated soot. Calcium seems to be more in the bulk than in the surface, because it is not observed in spectra recorded with the surface sensitive LAMPAS instrument. Elements such as sodium, chlorine and potassium show no significant differences between the two types of soot. Only slight, but not significant differences were obtained between the two examined size classes of the particles of the first and second impactor stages.

In a next step, the elemental depth distribution of the soot particles was investigated. The depth distribution of the recorded elements C, Hc (determined from CH cluster), S, Cl, N, Na shows weak, however significant differences between the two types of soot in the region near the surface of about 30 nm (see Fig. 6b–d). All non-carbon elements are only detected at the vicinity of the surface. All soot particles have a surface layer of organic hydrogen, which appears to be somewhat thicker in the case of sampling after the denuder from the same engine. Moreover, both diesel soot

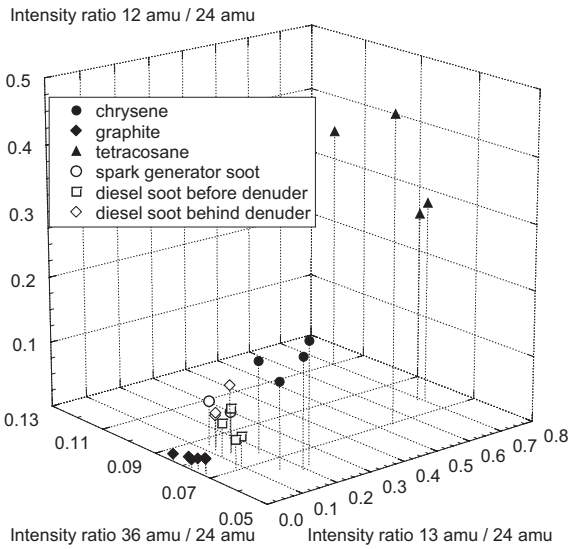

Fig. 7. Comparison of the mass signal patterns of carbon containing sputtered ions of diesel soot and spark generated soot (QMS-SIMS with negative polarity). With the intensity ratios (12 amu/24 amu, (13 amu/24 amu) and (36 amu/24 amu) the carbon chemistry can be classified into graphite, condensed aromatic hydrocarbons, aliphatic hydrocarbons and compounds with singular carbon atoms.

particle samples contain slightly more nitrogen in the surface region than the spark generated soot which is probably due to reactions with NO_x in the exhaust gas. The particle core almost only contained carbon. However, the diesel soot particles showed more sulfur in deeper regions than the soot particles from the spark generator.

Generally, the chemical state of carbon can be analyzed based on a signal pattern analysis of four intensities on the masses 12 amu (C^-), 13 amu (CH^-), 24 amu (C_2^-) and 36 amu (C_3^-) in the negative SIMS mode. With the intensity ratios (12 amu/24 amu, (13 amu/24 amu) and (36 amu/24 amu) the carbon chemistry can be classified into graphite, condensed aromatic hydrocarbons, aliphatic hydrocarbons and compounds with singular carbon atoms (Bentz, Fichtner, Goschnick, Häcker, & Ache, 1994). According to these intensity relations the comparison of spark generated soot and diesel soot show only slight differences in the chemical state of carbon in the surface region of about 30 nm (see Fig. 7). In all cases the carbon seems to be a mixture of graphitic carbon embedment and organic carbon in annular ring structures.

In the negative ion spectra the diesel soot particles show a higher ratio of the intensities for 80 amu (SO_3^-)/24 amu (C_2^-) and 96 amu (SO_4^-)/24 amu (C_2^-) than spark generated soot. This indicates a higher concentration of sulfate in the diesel soot that is consistent with the higher sulfur concentration indicated by the SNMS spectra and depth profiles.

3.4. Photo electron spectroscopy (XPS)

XPS was employed to analyze the chemical embedment of the surface carbon and surface sulfur. The C1s-Peak, which was fitted with the four components graphite, CH, C–O, and O–C–O showed no significant difference in the area ratio of the four components between the two types of soot.

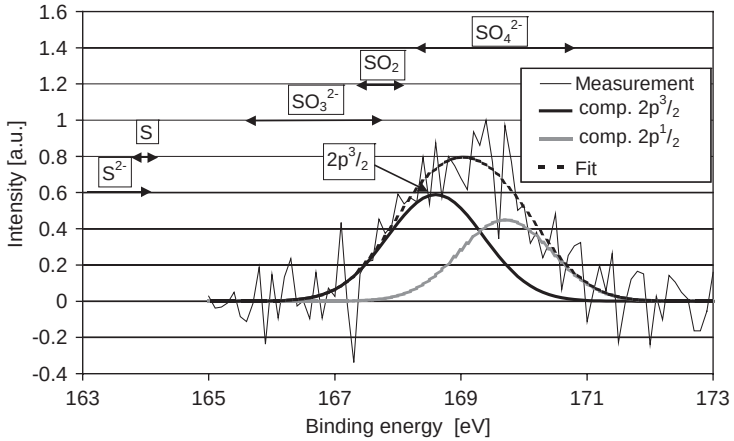

Fig. 8. XPS spectrum of a diesel soot sample in the S2p region: Sulfur was found to occur exclusively as sulfate (oxidation state +6) at the surface of the soot particles. The arrows show the characteristic binding energy ranges of the S2$p^{3/2}$ peak for possible chemical states of sulfur (Moulder et al., 1992).

Moreover, sulfur could only be detected in its highest oxidation state (i.e. +6) for diesel soot particles. This is in agreement with the results of XPS-investigations of diesel engine exhaust particles of Albers et al. (2000) where exclusively sulfate-bound sulfur was found in the diesel soot particles after passing the exhaust gas oxidation catalyst. In the spark generated soot particles near the surface the sulfur content was under the detection limit of XPS. This is confirmed by the higher sulfur content found by SNMS for the diesel soot. Fig. 8 shows an XPS-spectrum of the sulfur 2p peak with the two duplet components $2p^{3/2}$ and $2p^{1/2}$ of a diesel soot sample. The energy ranges marked with arrows belong to possible chemical states of sulfur binding energies of the S$2p^{3/2}$ component according to Moulder, Stickle, Sobol, and Bombon (1992). It is obvious that the sulfur can be exclusively assigned to sulfate. Almost all other elements were under the detection limit of XPS, which is generally about 1 atom% for an information depth of about 10 nm.

4. Analysis of diesel soot—$(NH_4)_2SO_4$—mixtures

Two sets of experiments (Nos. 5 and 6) were performed to investigate coagulation of diesel soot and ammonium sulfate particles. In the first set of experiments 140 μg m^{-3} ammonium sulfate were mixed with 50 μg m^{-3} diesel soot and were allowed to age for 26 h at a relative humidity of 45–36%. In the second series 1500 μg m^{-3} ammonium sulfate were mixed with 100 μg m^{-3} diesel soot and allowed to age for 45 h at a relative humidity of 46–37%. In the second experiment the ratio of diesel soot mass to ammonium sulfate mass content was changed from 36% to 7%.

4.1. Single particle mass spectrometry

The LAMPAS detection efficiency of pure ammonium sulfate particles is low, because ammonium sulfate does not absorb sufficient light at the ionization wavelength of 337 nm to produce detectable

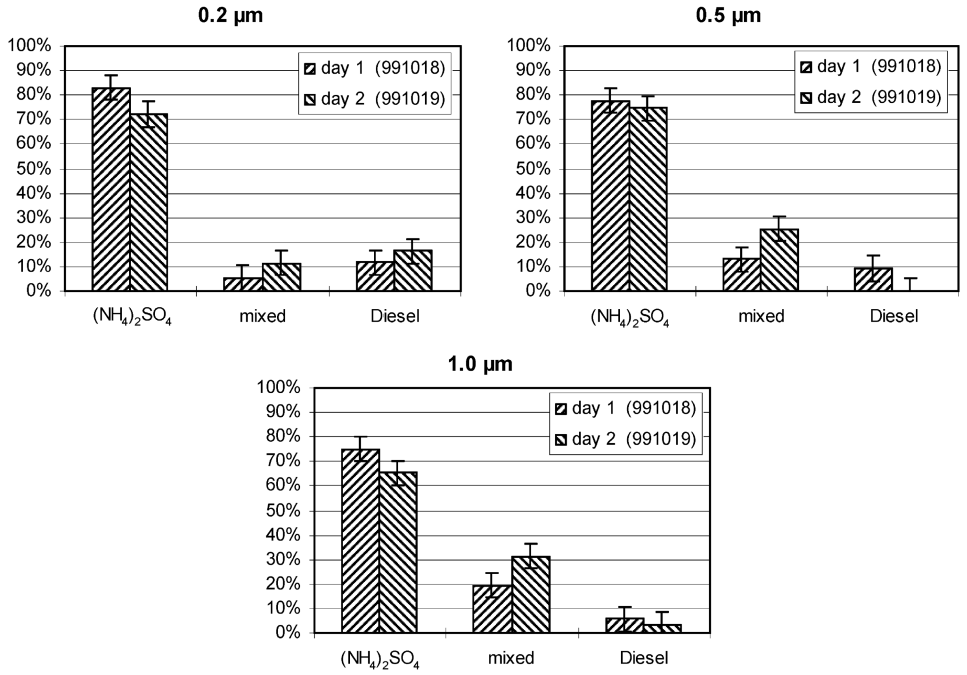

Fig. 9. Aerosol mixing: experiment No. 5 (140 µg m^{-3} ammonium sulfate +50 µg m^{-3} diesel soot). Fraction of ammonium sulfate, diesel soot, or internally mixed particles at three sizes shortly after mixing of the neat components (day 1), and ~20 h later (day 2). The error bars are due to omitted or wrongly classified spectra.

ions. Ionization most likely occurs because of impurities in the surface region. The ion Na^+ at 23 amu occurs as the most intense signal (ammonium sulfate Suprapur, Merck Darmstadt, Germany contains up to 0.1 ppm sodium). Because of the high sensitivity of the instrument for surface adsorbates, the mass spectra of ammonium sulfate and diesel soot were quite similar, although their bulk composition is very different, which makes the distinction between an external and an internal mixture very difficult. A small signal (< 10% full scale) of HSO_4^- at 97 amu and oxygen free carbon cluster fragments from an organic impurity are observed in some ammonium sulfate particles, but no K^+, which is present in all diesel soot particles. All these spectra without K^+ signals are attributed to ammonium sulfate particles. Spectra containing both, K^+ and carbon clusters, or K^+ and large Na^+ are considered to be mixed particles. All other K^+ containing particles are attributed to diesel soot.

In the second experiment the change of the ratio of ammonium sulfate mass to diesel soot mass from 36% to 7% is qualitatively confirmed by the larger fraction of spectra attributed to ammonium sulfate and the smaller fraction attributed to diesel soot compared to the first series of experiments (Figs. 9 and 10). Therefore, the tentative assignment of spectra to different types of particles appears to be correct.

In the first experiment three sizes of particles, i.e. 0.2, 0.5, and 1.0 µm were analyzed after filling the aerosol into the chamber (at $t = 2$ h; day 1) and after ~20 h (day 2). The percentage of mixed particles increased from day 1 to day 2, however within the error limits (see below), the decrease of

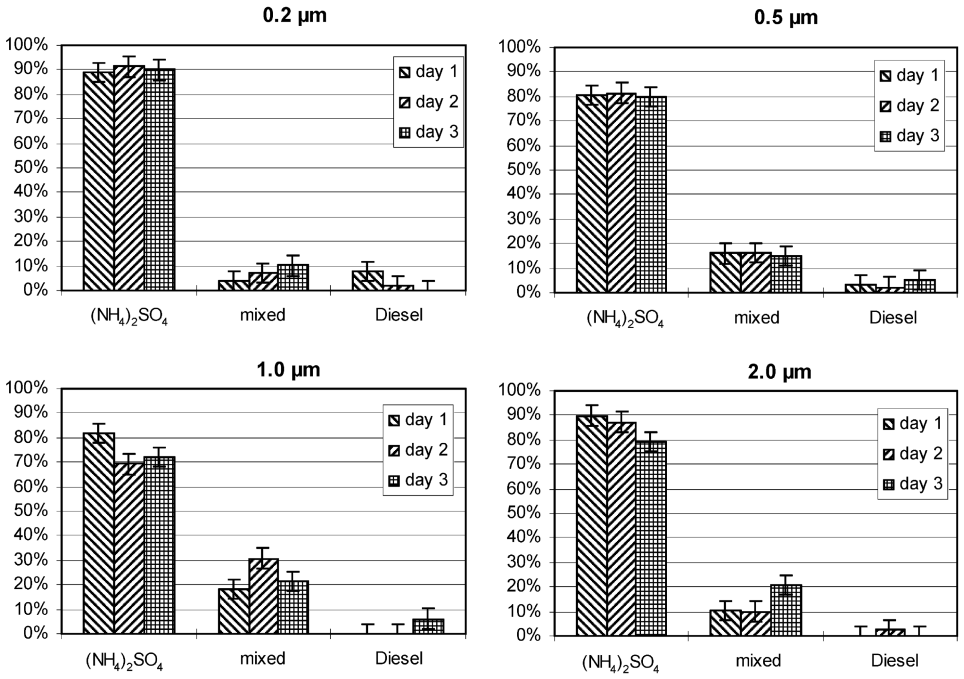

Fig. 10. Aerosol mixing: experiment No. 6 (1500 µg m^{-3} ammonium sulfate +100 µg m^{-3} diesel soot). Fraction of ammonium sulfate, diesel soot, or mixed particles at four sizes shortly after mixing of the neat components (day 1), after ~20 h (day 2), and after ~40 h (day 3).

ammonium sulfate and diesel soot is very small (Fig. 9). The relative increase of mixed particles is more predominant with increasing particle size, which is expected because mixed particles are larger. There are 5–10% mixed particles at 0.2 µm, 10–25% at 0.5 µm, and 20–30% of the particles are mixed at 1.0 µm. The temporal change during the experiment is less than the change with particle size. SMPS measurements show that the absolute amount of small particles decreases and the number of larger particles increases due to coagulation (Wentzel et al., 2003).

Usually, ~300 particle spectra were recorded for each classification. The error bars (Figs. 4, 9, and 10) are set to ± 5%, corresponding to ~15 spectra, which are not classified by the fuzzy clustering software and therefore are omitted, or which are sorted into the wrong class of spectra.

In the second experiment it was possible to measure four sizes, i.e. 0.2, 0.5, 1.0, and 2.0 µm aerodynamic diameter, during the three days of the experiment (at $t = 1$, 17, and 31 h). If compared to the first experiment, the increase of mixed particles with time seems to be even smaller. Due to the higher aerosol concentration a faster coagulation is expected. The relative amount of mixed particles increases from 5% to 15% at the beginning of the experiment to 10–20% at the end. Mixed particles are more abundant among the large sizes 0.5, 1.0, and 2.0 µm, and diesel soot particles of 1.0 or 2.0 µm aerodynamic diameter are virtually not observed. It was also observed by hygroscopicity measurements with a HTDMA (E. Weingartner, private communication; Saathoff et al. (2003c)) that the aerosol contains a significant fraction of non-hygroscopic, i.e. only soot containing particles after 23 h. The size distribution of diesel soot has its number maximum around 0.1 µm

and therefore, diesel soot can only be found in larger size classes as mixed particles with large ammonium sulfate particles. All of the largest particles are mixed particles or excess ammonium sulfate particles. Although the relative amount of mixed and neat particles is constant, the absolute amount of large particles increases to the expense of small particles, and therefore more mixed particles are created, which is consistent with SMPS measurements (Wentzel et al., 2003). The given percentages for mixed particles are very uncertain due to the missing absorption of ammonium sulfate at the ionization laser wavelength of 337 nm and the resulting difficulties to discriminate between ammonium sulfate and diesel soot particles as described above. However, it can be concluded that a significant portion of the aerosol is still externally mixed.

A comparison with TEM/EDX measurements by Wentzel et al. (2003) is consistent with the number of mixed particles in experiment 5. In experiment 6, Wentzel et al. report qualitatively the same observations with formation of more mixed particles during experiments No. 5 and No. 6. Also, the amount of neat ammonium sulfate particles measured by TEM/EDX is much lower in both experiments. Differences may also be due to the size range of 100 to 1500 nm, which was taken into account. Also, in TEM/EDX experiments the geometrical size is obtained, whereas the aerodynamic diameter is used in Single Particle MS experiments.

5. Investigation of coated soot aerosol particles

In the experiments No. 7 and 9,80 $\mu g\,m^{-3}$ diesel soot or 110 $\mu g\,m^{-3}$ spark generated soot were filled into the aerosol chamber and ~470 ppbv ozone were added. After complete mixing, 60 ppbv α-pinene were added and the formation of new particles was observed in the size distribution in experiment No. 7, but much less in experiment No. 9. Well-known products of the reaction of ozone with α-pinene are pinic acid, pinonic acid, and nor-pinic acid, which have low vapor pressures and may form new particles (Hoffmann, Bandur, Marggraf, & Linscheid, 1998), or may condense onto the soot particles (Saathoff et al., 2003c).

5.1. Single particle mass spectrometry

In both experiments most of the newly formed particles are too small, i.e. < 0.15 μm aerodynamic diameter, to be detected by the LAMPAS. Many of the larger particles cause a light scatter signal, but because the formed organic material does not absorb efficiently at 337 nm, no ions were formed and the resulting empty spectra were discarded. Also, due to the organic coating on soot the particle scattering albedo is increased (Saathoff et al., 2003c) and thus their ionization efficiency decreases.

In the diesel soot experiment No. 7, some soot particles could still be detected and additionally new fragments of oxygen containing hydrocarbons ($C_2H_3O^+$ at 43 amu, $C_3H_3O^+$ at 55 amu, $C_3HO_2^+$ at 69 amu, $C_4H_3O_2^+$ at 83 amu, $C_3H_5O_2^-$ at 73 amu, and C_6HO^- at 89 amu as the largest new peak) were observed (Fig. 11a). The new signal of C_6HO^- at 89 amu appears in the negative spectrum of each particle, indicating that all particles were coated during the experiment. No differences between particles of different sizes were observed. In a control experiment, diesel soot was treated with ozone and only a small increase of some oxygen containing hydrocarbon fragments was observed, but clearly no signal of C_6HO^- at 89 amu appeared. Apparently, it is characteristic for the reaction products of α-pinene and ozone and has also been observed in other studies (Hoffmann et al., 1998).

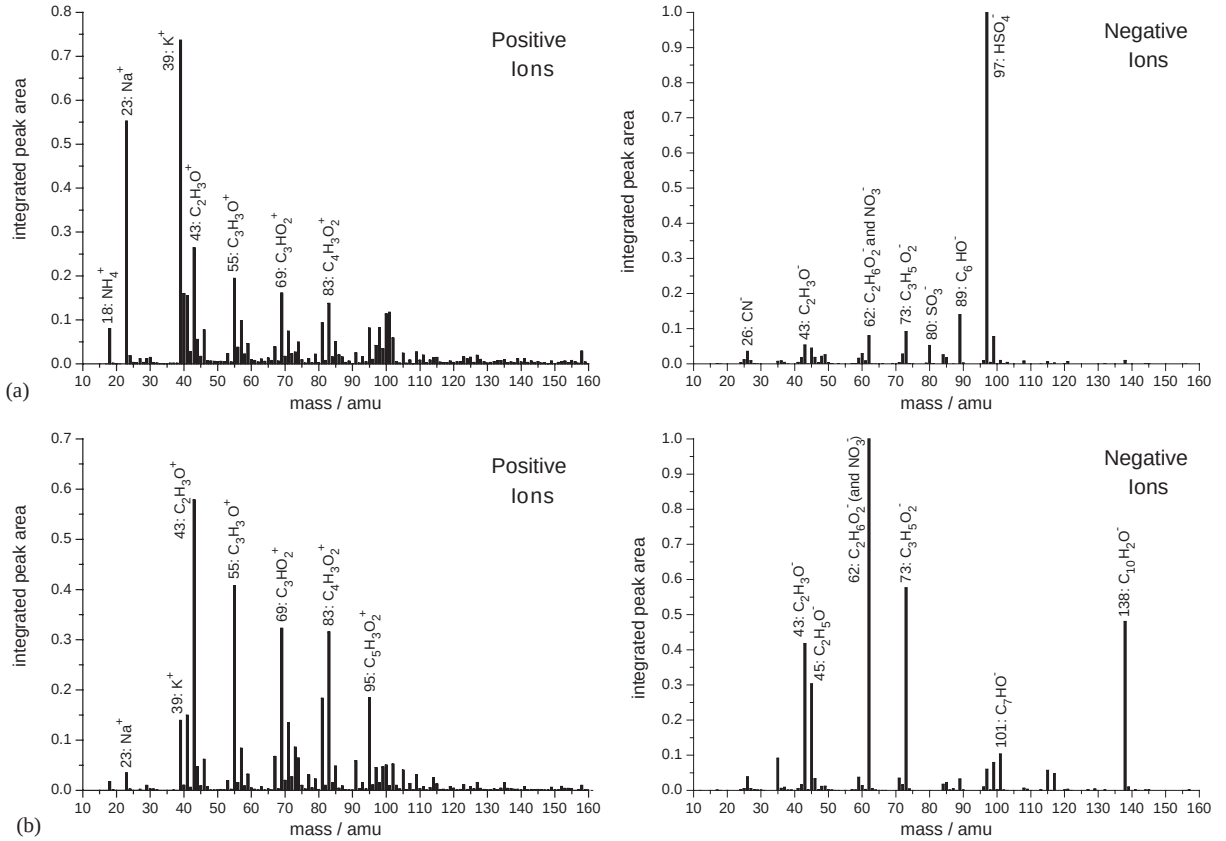

Fig. 11. (a) Class of spectra obtained from 0.5 μm diesel soot particles, which were coated with the reaction products of ~470 ppbv ozone and 60 ppbv α-pinene in the aerosol chamber and (b) class of spectra from 0.5 μm spark generated soot particles, which were coated under the same conditions.

Hoffmann et al. (1998) observed large fragment ions, mainly with masses >100 amu, because the authors evaporated the particles and ionized the resulting gases with a corona discharge, whereas the Single Particle Mass Spectrometer uses photo ionization of material that is adsorbed on a soot matrix.

The experiment No. 9 with spark generated soot aerosol was carried out analogously to the diesel soot experiments. Again, a coating was observed on all soot particles (Fig. 11b), but the spectral composition of the coating was distinctly different when compared to the coating on diesel soot (Fig. 11a). The intensity of the positive fragments $C_2H_3O^+$ at 43 amu and $C_3H_3O^+$ at 55 amu was increased, and the new fragments $C_3HO_2^+$ at 69 amu, $C_4H_3O_2^+$ at 83 amu, and $C_5H_3O_2^+$ at 95 amu appeared. In negative ion mode, the intensity of $C_3H_5O_2^-$ at 73 amu increased and several new peaks were observed: $C_2H_3O^-$ at 43 amu, $C_2H_5O^-$ and CO_2H^- at 45 amu, C_7HO^- at 101 amu, and $C_{10}H_2O^-$ at 138 amu. These peaks are attributed to fragments of the coating of α-pinene oxidation products. The peak at 89 amu was observed only with a very low intensity in spark generated soot.

The difference of the spectra of the coatings may be due to a matrix effect, i.e. different ionization processes on diesel soot or spark generated soot, resulting in different fragments from the same

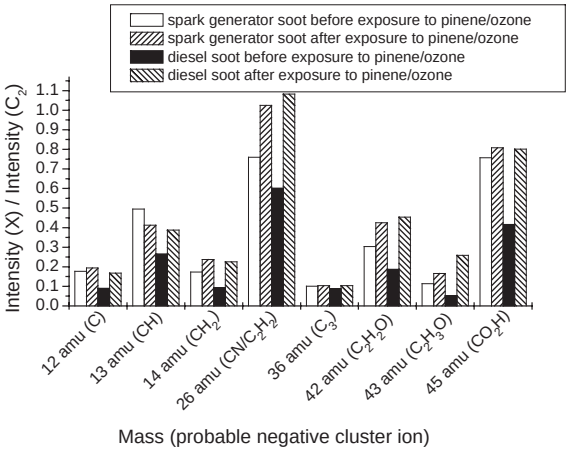

Fig. 12. QMS-SIMS of negative ions: signal intensities of carbon and carbon containing clusters typical of hydrocarbon compounds and their oxidation products before and after exposure of soot particles to α-pinene and ozone.

adsorbed compound. Also, a layer thickness of 2–4 nm for the coating on spark generated soot and of 7–11 nm on diesel soot particles have been estimated (Saathoff et al., 2003c). For diesel soot the same amount of material is adsorbed on a smaller surface area which may influence the ionization process. A less likely, but still possible explanation would be, that the different spectra could arise from different reaction products that are preferentially adsorbed on either type of soot due to the different surface characteristics of both types of uncoated soot particles (Fig. 3a, b and d). However, clearly coating of all particles was observed. All fragments originate from the ionization of known α-pinene oxidation products such as pinic acid, pinonic acid, and nor-pinic acid. A small, but significant peak at 187 amu (not shown) is observed on both types of soot and may be attributed to pinic acid-H^-, $C_9H_{15}O_4^-$.

5.2. Plasma-based SNMS and QMS-SIMS

At first using SNMS depth profiling no significant changes were observed in the characteristic elemental and cluster signals of both types of soot before and after the exposure to α-pinene and ozone. However the change in surface composition due to exposure to α-pinene and ozone was detected with the other methods Single Particle MS, TOF-SIMS and XPS. Obviously, the specific analytical conditions using plasma based SNMS lead to an insufficient sensitivity to detect the change of the surface composition.

The SIMS spectra of the surface region (depth up to 30 nm) of the soot particles showed a clear increase of cluster signals typical for oxidation products of organic compounds (Fig. 12). In the negative SIMS mode a rise of the intensities of the signals at 42 amu ($C_2H_2O^-$), 43 amu ($C_2H_3O^-$), and 45 amu (CO_2H^-) can be observed, which is larger than the rise of other peaks of the spectra. In agreement with the single particle mass spectra (Fig. 11b) the positive secondary ions at masses 43 amu ($C_2H_3O^+$) and 55 amu ($C_3H_3O^+$) showed the highest intensity increase. Diesel soot showed a qualitatively higher increase of the cluster signals typical for oxidation products.

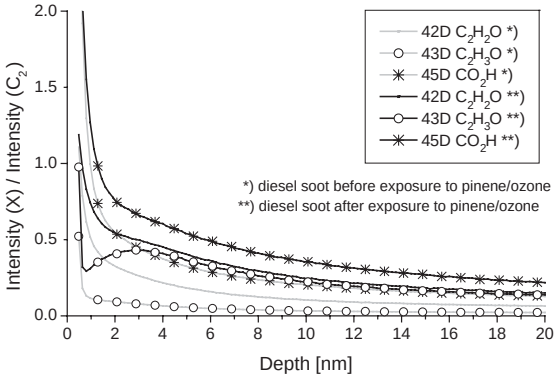

Fig. 13. QMS-SIMS of negative ions: Depth profile of cluster signals of oxygen containing hydrocarbons before and after exposure of diesel soot particles to α-pinene and ozone. Sputter time was converted into a depth scale with an erosion rate of 0.05 nm/s for the soot particles (see text). Every fifth data point is marked with a symbol.

Determination of the layer thickness is in this case difficult with SIMS, because of the high irregularity of the particles. The ion bombardment at a tilted angle of 60° to the sample surface causes shadowing effects and uneven erosion. The diesel soot particles exhibit a layer structure according to depth profiles of mass 43 amu (C_2HO^+) (see Fig. 13). The layer does not exceed a depth of 10 nm. However, this laminated structure was far less pronounced in the SIMS depth profile of spark generated soot. This is in agreement with the findings of Saathoff et al. (2003c) who estimated a thicker layer on diesel soot in comparison to spark generator soot. After the exposure of the spark generated soot particles to α-pinene and ozone slightly higher but almost constant intensities of cluster signals typical for oxidation products of organic compounds point to evenly distributed acid derivatives also in greater depth of the particles.

5.3. TOF-SIMS

For a more detailed analysis spectra were acquired with the TOF-SIMS-instrument, which was used in the static SIMS mode. Additional fragments of high molecular mass appeared in the spectra in comparison to dynamic SIMS. The molecular ions of the three oxidation products pinonic acid, pinic acid and nor-pinic acid were recorded (see Fig. 14b), which were particularly strong in the case of diesel soot particles. Measurements of pinic acid and pinonic acid, obtained as commercial standards, confirmed that the acid derivatives emit the so-called M-H-ions on the nominal masses 185 amu ($C_9H_{13}O_4^-$, pinic acid) and 183 amu ($C_{10}H_{15}O_3^-$, pinonic acid) which were all found in the spectra of soot after exposure to ozone/α-pinene. Additionally, smaller cluster signals typical of oxidation products were observed for the coated particles (see Fig. 14a).

5.4. Photo electron spectroscopy (XPS)

XPS was applied in order to further characterize the chemistry of carbon in the surface region up to 10 nm of the soot particles. XPS spectra of soot particles were recorded before and after exposure to α-pinene and ozone. The C1s signal group was fitted assuming a four-component signal for the

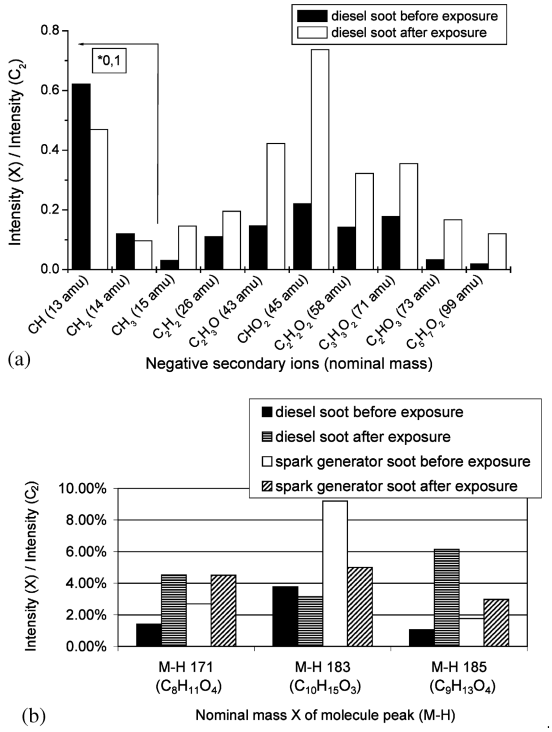

Fig. 14. TOF-SIMS of negative ions: (a) Cluster signals of oxygen containing hydrocarbons before and after exposure of diesel soot particles to α-pinene and ozone; (b) Fragment signals before and after exposure that can be assigned to the M-H peaks of acid derivatives of α-pinene and ozone.

chemical states of carbon, i.e. graphite, CH, C–O, and O–C–O. Significantly higher intensities of C–O and O–C–O components in relation to the graphite component intensity were observed after exposure to α-pinene and ozone compared to the initial state, particularly in the case of diesel soot (see Fig. 15).

6. Conclusions

Diesel soot and spark generated soot were analyzed by different surface sensitive analysis methods. Further, the mixing of aerosols, i.e. diesel soot and ammonium sulfate aerosol, and exposure of diesel soot or spark generated soot to α-pinene and ozone were investigated. Photo-ionization of individual particles, which is utilized in the single particle mass spectrometer (LAMPAS 2) is a surface sensitive process. The observed differences of the mass spectra of both types of soot indicate a difference in the chemical surface composition. The spark generated soot was sampled after dilution with dry air, and after dilution with 60 ppbv NO_x containing humidified air for comparison to diesel soot. An obvious difference in the obtained spectra was a larger signal of NO_x reaction products on the soot surface, but the main differences between diesel soot and spark generated soot remained. Investigations with plasma-based SNMS, QMS-SIMS, TOF-SIMS and XPS of the soot samples taken directly from the

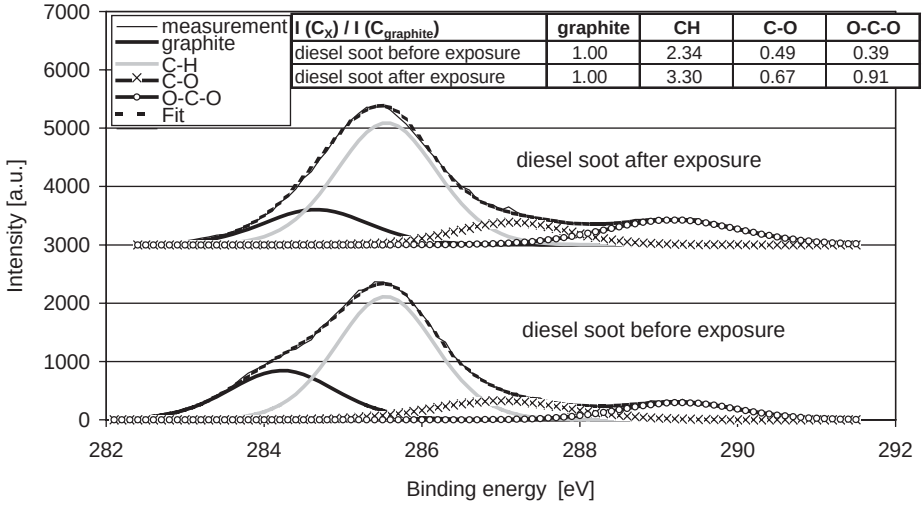

Fig. 15. XPS-spectrum of diesel soot in the C1s region: Measured signal (solid) and fitted signal components (dashed) for C-C, C-H, C-O and O-C-O carbon chemical embedment. An increase of the C-O and O-C-O component can be seen for the soot particles after exposure to α-pinene and ozone.

sources revealed the following differences: The diesel soot particles clearly show a higher content of sulfur compared with the spark generated soot. The sulfur mainly occurs in its highest oxidation number (+6, e.g. sulfate). Additionally, a higher content of NH_4^+ was found for diesel soot particles in FTIR spectra which might partially originate from neutralization of H_2SO_4 by ambient ammonia during sample handling. Likewise, the concentration ratio of carbon-bound hydrogen to carbon is higher in diesel soot than in spark generated soot. Therefore, different atmospheric reactivity for the two types of soot would not be surprising, since chemical interactions between particles and gases are expected to be primarily influenced by the particle surface composition.

During mixing experiments of diesel soot and ammonium sulfate aerosol, the single particle MS spectra did not allow unambiguous attribution of neat diesel, neat ammonium sulfate, or mixed particles. The diesel spectra often contained large signals of sulfate, which was formed in the engine due to oxidation of the fuel sulfur. On the other hand, the ammonium sulfate spectra contained carbon fragments from an organic impurity. This made the spectra of both types of aerosol very similar and difficult to separate, although the main composition is quite different. A qualitative assessment of the data reveals a higher number of mixed particles at larger sizes (0.5 μm aerodynamic diameter and above) than at small sizes (0.2 μm). Only a relatively small increase of internally mixed particles was observed (∼5%). Therefore, it is concluded, that most of the observed internal mixing was completed within the first hours of the experiments before the spectra were recorded and that further internal mixing is slow (Wentzel et al., 2003).

Due to the surface sensitivity, photo-ionization single particle mass spectrometry is well suited to investigate surface changes of particles. A coating on the surface of all soot particles was observed after addition of ozone and α-pinene to either diesel soot, or spark generated soot aerosol in the chamber. The spectra of the coatings on diesel soot and on spark generated soot differed, which may

be due to different ionization processes, or less likely, due to the adsorption of two different reaction products on either type of soot.

A coating of the particles of both types of soot could be confirmed by investigations with the QMS-SIMS, TOF-SIMS and XPS: QMS-SIMS spectra show considerably increased cluster signals of oxidation products of hydrocarbons after exposure to α-pinene and ozone. The oxidation products were identified as the acid derivatives of α-pinene based on data of TOF-SIMS. A comparison of XPS-spectra before and after the α-pinene/ozone exposure shows a rise of the C–O and the O–C–O components of the C1s-signal group. Diesel soot particles were generally found to develop a more pronounced layer of the acid derivatives of the α-pinene than the spark generated soot particles.

This investigation clearly revealed differences in the surface composition of diesel soot particles and spark generated soot particles. It is also shown, that different analytical techniques with distinct capabilities display in principal the same characteristic properties of both types of soot particles.

Acknowledgements

This work was partially supported by the BMBF within grant 07AF210A. We like to thank Prof. B. Spengler, Dr. P. Hinz and A. Trimborn, for the collaboration in building the single particle mass spectrometer. Also, we would like to thank Prof. A. Benninghoven and his coworkers R. Kamischke and F. Kollmer (Westfälische Wilhelms Universität Münster) for the support during the measurements with the TOF-SIMS instruments. Additionally, we thank M. Bruns and H. Deutsch (Forschungszentrum Karlsruhe) for the support with the XPS measurement.

References

Albers, P. W., Klein, H., Lox, E. S., Seibold, K., Prescher, G., & Parker, S. F. (2000). INS-, SIMS- and XPS-investigations of diesel engine exhaust particles. *Physical Chemistry Chemical Physics*, *2*, 1051–1058.

Ammann, M., Kalberer, M., Jost, D. T., Tobler, L., Rössler, E., Piguet, D., Gäggeler, H. W., & Baltensperger, U. (1998). Heterogeneous production of nitrous acid on soot in polluted air masses. *Nature*, *395*, 157–160.

Bentz, J. W. G., Ewinger, H.-P., Goschnick, J., Kannen, G., Ache, H.-J. (1993). Depth-profiling of organic layers on microparticles with SNMS. *Fresenius' zeitschrift fuer Analytische chemie*, 346, 323.

Bentz, J. W. G., Fichtner, M., Goschnick, J., Häcker, C.-J., & Ache, H.-J. (1994). Chemical characterisation in depth-profiling of organic material by evaluation of small molecular secondary ions. Part II: Recognition of hydrocarbon structure of organic compounds. In: A. Benninghoven et al. (Eds.), *Secondary Ion Mass Spectrometry SIMS IX* (pp. 768). New York: Wiley.

Berner, A., & Klaus, N. (1985). *Staub Reinhaltung der Luft*, *45*(4), 168–170.

Ewinger, H. P., Goschnick, J., & Ache, H-J. (1991). Analysis of organic compounds with SNMS. *Journal of the American Society of Mass Spectrometry*, *341*, 17.

Goschnick, J., Schuricht, J., & Ache, H-J. (1994). Calibration of depth profiles of microparticles measured with plasma-based secondary neutral mass spectrometry. *Fresenius' zeitschrift fuer Analytische Chemie*, *349*, 203.

Goschnick, J., Schuricht, J., Schweicker, A., & Ache, H-J. (1993). Sputter yields and erosion rates for low energy bombardment of multielemental powders. *Nuclear Instruments Methods in Physical Research*, *B83*, 339.

Gross, D. S., Gälli, M. E., Silva, P. J., & Prather, K. A. (2000). Relative sensitivity factors for alkali metal and ammonium cations in single-particle aerosol time-of-flight mass spectra. *Analytical Chemistry*, *72*, 416–422.

Hinz, K. P., Greweling, M., Drews, F., & Spengler, B. (1999). Data processing in on-line laser mass spectrometry of inorganic, organic, or biological airborne particles. *Journal of the American Society of Mass Spectrometry*, *10*, 648–660.

Hoffmann, T., Bandur, R., Marggraf, U., & Linscheid, M. (1998). Molecular composition of organic aerosols formed in the α-pinene/O_3 reaction: Implications for new particle formation processes. *Journal of Geophysical Research*, *103*, 25569–25578.

Jede, R., Seifert, K., & Dünnebier, G. (1987). Combined electron gas SNMS and SIMS instrument for trace and depth profile analysis with high dynamic range. *Fresenius' Zeitschrift fuer Analytische Chemie*, *329*, 116–121.

Kamm, S., Möhler, O., Naumann, K. H., Saathoff, H., & Schurath, U. (1999). The heterogeneous reaction of ozone with soot aerosol. *Atmospheric Environment*, *33*, 4651–4661.

Kirchner, U., Börensen, C., Scheer, V., & Vogt, R. (1999). An FTIR study of soot and mineral dust model compounds and selected reactions with nitrogen oxides. In: P. M. Borrell & P. Borrell (Eds.), *Proceedings of the EUROTRAC symposium '98*, Vol. 1 (pp. 666–670). Southampton: WIT Press.

Kirchner, U., Scheer, V., & Vogt, R. (2000). FTIR spectroscopic investigation of the mechanism and kinetics of the heterogeneous reactions of NO_2 and HNO_3 with Soot. *Journal of Physical Chemistry*, *104*, 8908–8915.

Kirchner, U., Scheer, V., & Vogt, R. (2001). Heterogeneous reactions of soot with nitrogen oxides: An investigation by in-situ single particle mass spectrometry. In P. M. Borrell & P. Borrell (Eds.), *Proceedings of the EUROTRAC symposium 2000* Southampton: WIT Press (pp. 650–654).

Kotzick, R., Panne, U., & Niessner, R. (1997). Changes in condensation properties of ultrafine carbon particles subjected to oxidation by ozone. *Journal of Aerosol Science*, *28*, 725–735.

Moulder, J. F., Stickle, W. F., Sobol, P. E., & Bombon, D. E. (1992). In J. Chastain (Ed.), *Handbook of X-ray photoelectron spectroscopy*. Eden Prairie, Min., USA: Perkin Elmer Corporation.

Saathoff, H., Moehler, O., Schurath, U., Kamm, S., Dippel, B., & Mihelcic, D. (2003a). The AIDA soot aerosol characterisation campaign 1999. *Journal of Aerosol Science*, *34*, 1277–1296.

Saathoff, H., Naumann, K. H., Schnaiter, M., Schöck, W., Weingartner, E., Baltensperger, U., Krämer, L., Bozoki, Z., Pöschl, U., Niessner, R., & Schurath, U. (2003b). Carbon mass determinations during the AIDA soot aerosol campaign 1999. *Journal of Aerosol Science*, *34*, 1399–1420.

Saathoff, H., et al. (2003c). Coating of soot and $(NH_4)_2SO_4$ particles by ozonolysis of α-pinene. *Journal of Aerosol Science*, *34*, 1297–1321.

Schnaiter, M., Henning, T., Mutschke, H., Kohn, B., Ehbrecht, M., & Huisken, F. (1999). Infrared spectroscopy of nano-sized carbon grains produced by laser pyrolysis of acetylene: Analog materials for interstellar grains. *The Astrophysical Journal*, *519*, 687–696.

Schnaiter, M., Horvath, H., Möhler, O., Naumann, K.-H., Saathoff, H., & Schöck, O.W. (2003). UV-VIS-NIR spectral optical properties of soot and soot-containing aerosols. *Journal of Aerosol Science*, *34*, 1421–1444.

Shirley, D. A. (1972). High-resolution X-ray photoemission spectrum of the valence bands of gold. *Physics Review*, *B5*, 4709–4714.

Trimborn, A., Hinz, K-P., & Spengler, B. (2000). Online analysis of atmospheric particles with a transportable laser mass spectrometer. *Aerosol Science and Technology*, *33*, 191–201.

Weingartner, E., Burtscher, H., & Baltensperger, U. (1997). Hygroscopic properties of carbon and diesel soot particles. *Atmospheric Environment*, *31*, 2311–2327.

Weiss, M., Verheijen, P. J. T., Marijnissen, J. C. M., & Scarlett, B. (1997). On the performance of an on-line time-of-flight mass spectrometer for aerosols. *Journal of Aerosol Science*, *28*, 159–171.

Wentzel, M., Gorzawski, H., Naumann, K.-H., Saathoff, H., & Weinsbruch, S. (2003). Transmission electron microscopical and aerosol dynamical characterization of soot and ammonium sulfate/soot mixtures. *Journal of Aerosol Science*, *34*, 1347–1370.